Pergamon

0301-9322(95)00049-6

Int. J. Multiphase Flow Vol. 22, No. 1, pp. 195–201, 1996

0301-9322/96 $15.00 + 0.00

BRIEF COMMUNICATION

FLOODING IN A HORIZONTAL PIPE WITH BEND

S. WONGWISES

Department of Mechanical Engineering, Faculty of Engineering, King Mongkut's Institute of Technology Thonburi, 91 Suksawas 48, Bangmod, Radburana, Bangkok 10140, Thailand

(Received 3 February 1995; in revised form 11 June 1995)

1. INTRODUCTION

Flooding or countercurrent flow limitation (CCFL) have been studied both experimentally and analytically, mostly in vertical pipes (Bankoff & Lee 1983). Flooding in horizontal or nearly horizontal geometries has received comparatively little attention in the literature. Some of the earliest work was performed by Wallis & Dobson (1973), Gardner (1983) and Lee & Bankoff (1983). However, to study the phenomena of flooding in PWR hot legs, the results from CCFL studies in horizontal flow paths are not enough, this is due to the flow behavior near the bend connecting the horizontal pipe with the inclined riser which governs the CCFL characteristics of PWR hot legs (Ohnuki *et al.* 1988). There are only a few CCFL studies in an elbow geometry. Krowlewski (1980) studied the flooding limit of air–water in a horizontal pipe which was connected to a second pipe by a 45° or 90° elbow.

Siddique *et al.* (1986) measured the flooding limit in air–water countercurrent flow in elbows of a vertical upper limb and a lower limb, which was horizontal or slightly inclined. The effect of the tube diameter, the length and inclination of the lower leg of the elbow were examined. Wan (1986) conducted the experiments for CCFL of saturated steam and subcooled water in an upright 90° elbow. Kawaji *et al.* (1989) obtained air–water countercurrent flooding data for an elbow between a vertical and downwardly inclined pipe. Results are given for the experiments performed for different test elbows for different angles from 90° to 180° of a downwardly inclined pipe.

Relatively little information is currently available on countercurrent flow limitation, or flooding phenomena in horizontal pipes with a bend. In the present study, the main concern is to obtain the experimental results of CCFL of air and water in a bend between a horizontal pipe and a pipe inclined to the horizontal.

2. EXPERIMENTAL SET-UP AND PROCEDURE

A schematic diagram of the experimental system is shown in figure 1. Air and water are used as the working fluids. The main components of the system consist of the test section, the air supply, the water supply, the instrumentation and the data acquisition system. The test section, with an inside diameter of 64 mm, is made of transparent acrylic-glass to permit visual observation of the flow patterns. It is composed of a horizontal pipe, an upwardly inclined pipe and a bend which connects them. The inner and outer bend radii of curvature are 60 and 135 mm, respectively. The bends with different angles are constructed accurately by machining an ingot of acrylic-glass. The lower leg of the bend is connected to the horizontal pipe of which the other end is connected to the supply tank. The supply tank is a 400 mm diameter and 1060 mm tall cylindrical vessel. The length of the horizontal pipe can be varied during the experiments. The upper leg of the bend is connected to a straight pipe of 1300 mm length, the other end of which is connected to the water inlet section and the separation unit. The connections of the piping system are designed such that parts can be changed very easily. Air is injected from a compressor through the reservoir, regulation

valve, rotameter, supply tank and test section. Water is pumped from the storage tank through the rotameter, water inlet section, test section and supply tank and flows back to the storage tank. The entrained water is separated from the two-phase mixture by the cyclone separator and flows back to the storage tank. Two types of water inlet sections, namely an inner pipe inlet section and a porous inlet section, are used in the experiments. The inner pipe inlet section consists of a circular pipe of 32 mm inside diameter and 150 mm long which is installed in the pipe at the water inlet section. The porous section is made of sintered steel, 200 μm filter grade, and is 100 mm long. The water from the inlet section flows downward to the bend, the horizontal section and then to the supply tank, while the air flows countercurrently. The level of water in the supply tank is kept constant, and excess water is returned to the storage tank. The inlet flow rates of air and water are measured by two sets of rotameters. The entrained water flow rate is registered by two flow meters and returned to the storage tank, while the separated air is exhausted into the atmosphere. The pressure in the test section can be regulated and kept constant at 130 kPa automatically during the experiment by an absolute pressure transducer and a control valve in the air discharge line. The temperature of the air and water are measured by thermocouples. The two-phase pressure drop, between the supply tank and the upper part of the bend, is registered by a capacitive pressure transducer. Experiments are conducted with various flow rates of air and water, various inclination angles of the bend (Θ), various lengths of the horizontal pipe and various water inlet conditions. In the experiments the air flow rate is increased by small increments while the water flow rate is kept constant. After each change in inlet air flow rate, both the air and water flow rates are recorded. The experiments are carried out until the onset of liquid zero penetration appears, when all the water at the outlet is carried over by the air flow.

3. RESULTS AND DISCUSSION

Flooding may be characterized by visual observation and pressure drop. At specific experimental conditions the onset of flooding is found to depend on the inlet feed water flow rate.

Figure 2 shows the relation between the square root of the dimensionless superficial velocity of

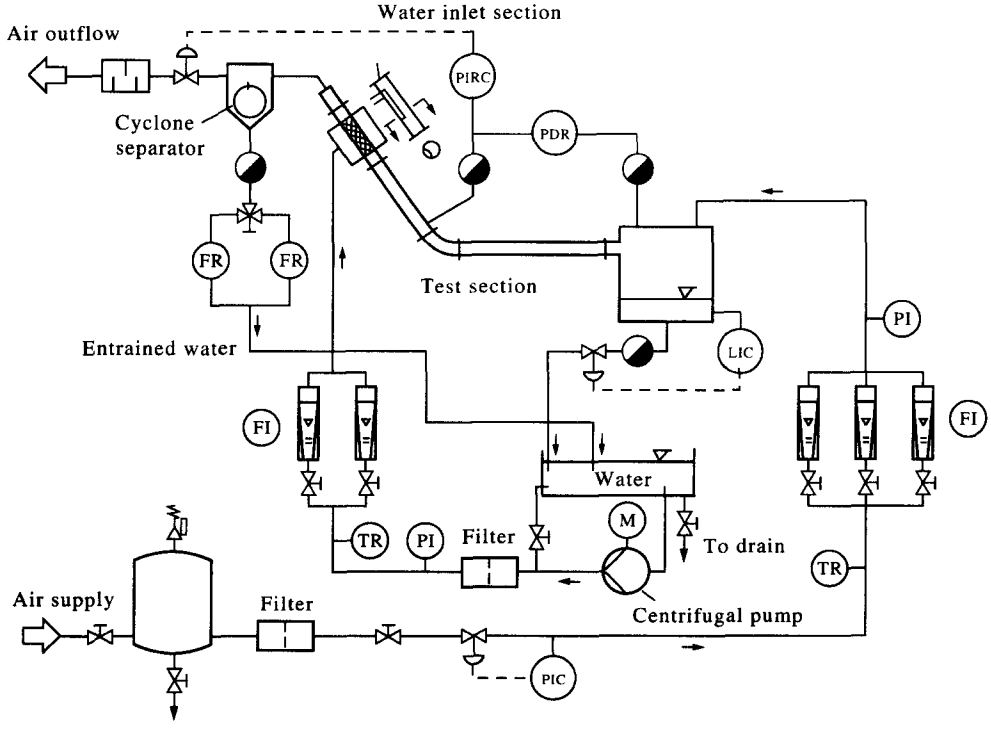

Figure 1. Schematic diagram of apparatus.

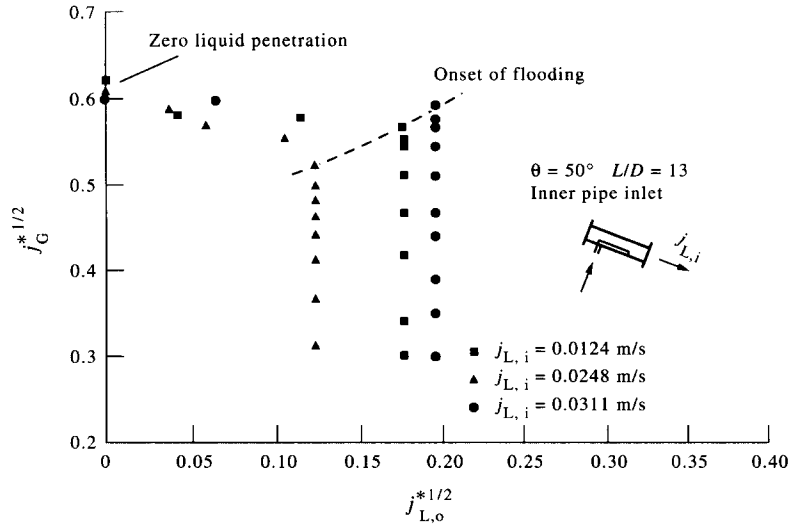

Figure 2. Relation between water outflow and air flow at constant inlet feed water flow.

water at the outlet of the horizontal pipe $(j_{L,o}^*)^{1/2}$ with the square root of the dimensionless superficial velocity of air $(j_G^*)^{1/2}$, respectively. The variables $(j_L^*)^{1/2}$ and $(j_G^*)^{1/2}$ are defined by:

$$j_k^* = j_k\left[\frac{\rho_k}{(\rho_L - \rho_G)gD}\right]^{1/2}$$

where j_k and ρ_k denote the superficial velocity and density of phase k respectively, g is the gravitational acceleration and D is the pipe diameter.

Before the onset of flooding is reached, the superficial velocities of the water phase at the inlet and at the outlet of the pipe are equal. The pressure drop of the two-phase flow increases slightly, until the onset of flooding is reached. Due to the instabilities at the interface, slugging occurs and the pressure drop suddenly increases. The slugs carry a fraction of the injected water to the outlet, the water flow at the outlet of the horizontal pipe is thus smaller and afterwards the pressure drop decreases.

A typical flooding curve connecting all points of the onset of flooding is shown in figure 3. It presents the relation between $(j_G^*)^{1/2}$ and $(j_L^*)^{1/2}$. The flooding curve is divided into three regions, in each of which the mechanism of flooding is different. These three mechanisms are dependent on the water flow rate.

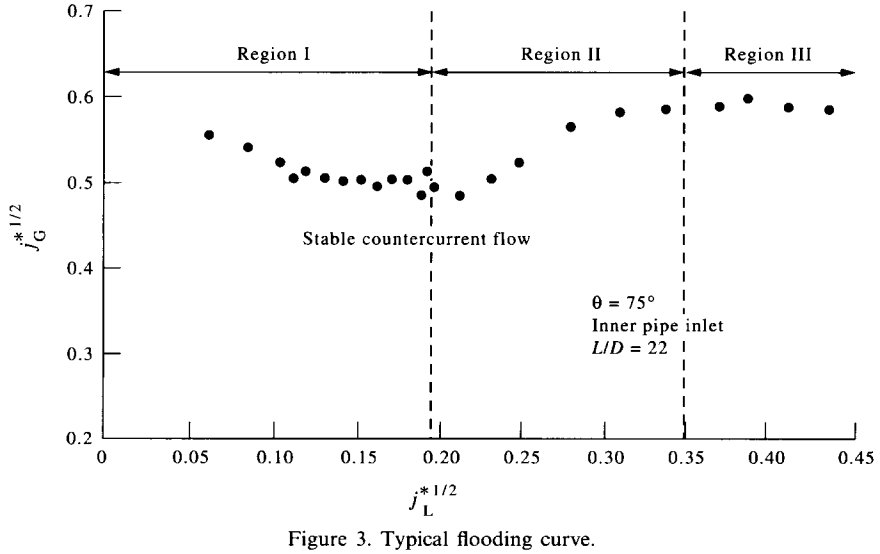

Figure 3. Typical flooding curve.

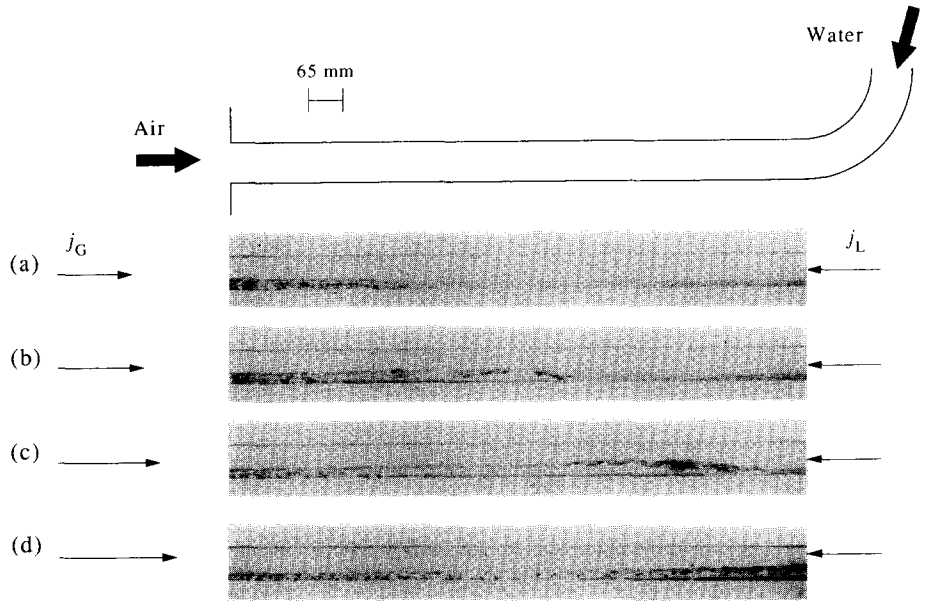

Figure 4. Flow pattern in a horizontal pipe in the first region of the flooding curve ($j_L = 0.0173$ m/s): (a) $j_G = 2.93$ m/s; (b) $j_G = 3.65$ m/s; (c) $j_G = 4.58$ m/s and (d) $j_G = 5.11$ m/s.

In the first region [$(j_L^*)^{1/2} < 0.2$], the air flow rate creating the onset of flooding decreases, while the water flow rate increases. Due to the water flow being accelerated by gravity, the supercritical flow suddenly changes to subcritical flow in the horizontal part and a hydraulic jump is observed (as shown in figure 4). The position of the hydraulic jump is dependent on the water flow rate. At low water flow rates, the hydraulic jump is very thin and appears near the bend. At higher water flow rates, the hydraulic jump is bigger and shifts away from the bend. With gradual increase of the air flow rate the hydraulic jump shifts in the direction of the bend. At a certain air flow the flooding point is reached. A large amplitude roll wave appears instead of a hydraulic jump. Air velocities near the crest of the waves are thus higher leading to the blowing up of the wave crests which break up into droplets and splash up the inner wall of the bend.

In the second region [$0.20 < (j_L^*)^{1/2} < 0.35$], the air flow rate which initiates flooding increases with the increase of the water flow rate. In this region two different phenomena are observed. For $(j_L^*)^{1/2}$ slightly greater than 0.20, the hydraulic jump occurs in the horizontal section near the supply tank and the height of the jump is higher as the air flow is increased.

Eventually, at a specific air flow rate, the onset of flooding is reached. The hydraulic jump passes upstream towards the bend, counter with the water flow. Due to the instability of the interface at the front face of the hydraulic jump, an unstable wave is formed. These waves join with the waves which are blown from the end of the horizontal leg and are moved in the direction of air flow. Occasionally the crests of the waves suddenly splash to the top of the wall inside the horizontal pipe. The flow area is reduced and the high velocity of the air pushes the injected water ahead like a froth-slug (as shown in figure 5). The formation of the slug is accompanied by a sharp rise in the pressure drop across the horizontal pipe and the slug leads to a continuous carry over of water from the horizontal pipe to the separation unit. Bridging of the pipe occurs inside the horizontal part near the bend before the slug moves through the bend to the inclined pipe. After the slug has passed, the water level in the horizontal pipe is reduced.

For $(j_L^*)^{1/2} > 0.20$, a slight increase in air flow causes the hydraulic jump to occur at the water outlet or somewhere near the outlet. Unstable waves are formed and splashed up to the upper wall of the horizontal pipe forming a slug. The slug is swiftly pushed upstream. Bridging occurs relatively far away from the lower leg of bend. In this region the location of the onset of flooding coincides with the one for the onset of slugging in the horizontal pipe, accompanied by partial or total carryover of the injected water.

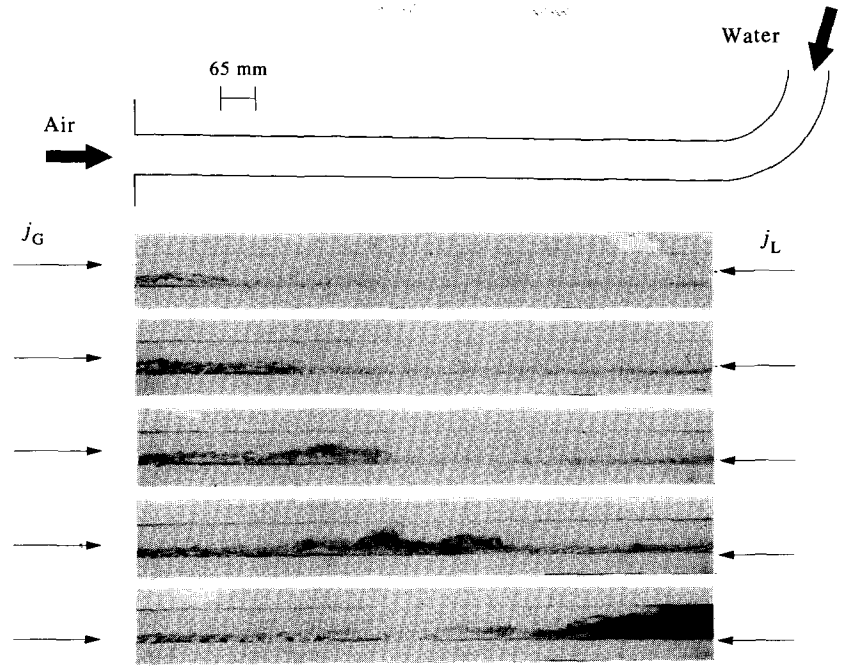

Figure 5. Flow pattern in a horizontal pipe in the second region of a flooding curve ($j_L = 0.0774$ m/s, $j_G = 6.88$ m/s).

In the third region, the water flow is large $[(j_L^*)^{1/2} > 0.35]$ and the air flow rate which initiates the flooding tends to decrease with increasing water flow rates. The flow is supercritical throughout the horizontal leg and no hydraulic jump is observed. As the air flow is gradually increased, the phenomena in the horizontal part are almost unchanged. Just before the onset of flooding, there is a thickening of the water film at the outlet. Many small droplets are carried back from the free water to the upper wall of the pipe near the outlet. At a sharply defined air flow rate, the slug is formed at the end of the horizontal pipe and blocks the whole tube section and is then pushed strongly by the air with very high velocity (as shown in figure 6) to the bend through the inclined pipe to the separation unit limiting the out-flow of water.

In figure 7, the flooding curves for the three pipes with different ratios of length to diameter are shown. With increasing horizontal pipe lengths, the air velocity at which flooding occurs decreases

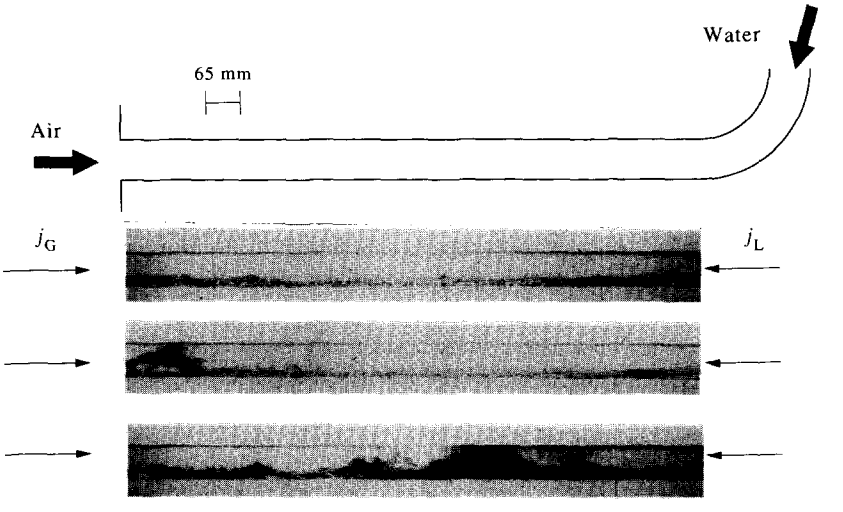

Figure 6. Flow pattern in a horizontal pipe in the third region of a flooding curve ($j_L = 0.1346$ m/s, $j_G = 7.06$ m/s).

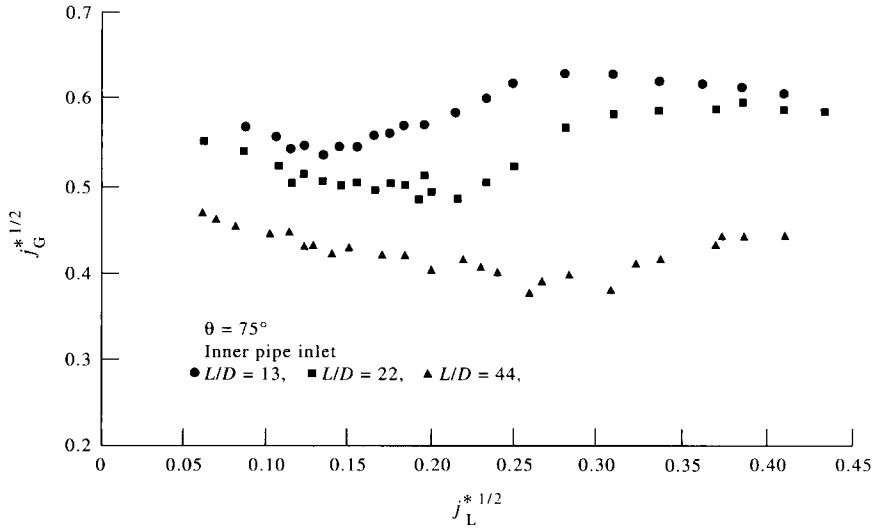

Figure 7. Effect of horizontal length on flooding.

for the whole range of water flow rate. Considering the first region of flooding curves for all pipe lengths, the water level at the connection between the bend and the horizontal part is larger for the case of the longer pipe. The height of the hydraulic jump is thus greater for a specific water flow. The air flow at the vicinity of the crest of hydraulic jump will be accelerated and thus has a higher air velocity leading to an earlier wave growth at the crest of the hydraulic jump and eventually flooding is initiated earlier. For shorter horizontal lengths, flooding in this region occurs at the interval which is narrower than in the case of the longer pipes. At intermediate water flow rates, a similar reason can be given. The influence of length becomes clearer in this region. The reason is due to the increase of friction when the pipe is longer, the water flow is decelerated and the liquid hold-up will be higher. The hydraulic jump is formed and flooding appears simultaneously with the onset of slugging somewhere in the horizontal part. At high water flow rates and for shorter pipes, the water flow rates create the supercritical flow through the horizontal part and the hydraulic jump is thus swept out from the end of the horizontal part and the mechanisms of flooding are changed to the formation of slugging at the end of horizontal pipe. This requires much higher air flow rates to initiate flooding than the longer horizontal lengths at the same water flow and the lower water flow rate at the same pipe lengths. It can also been seen that the influence of length becomes more clear when the water flow is larger.

4. CONCLUSION

Flooding or countercurrent flow limitation (CCFL) determines the maximum flow rate of one phase which can flow countercurrently to another phase. In the present study, the experimental data of the countercurrent flow limitation for air and water in a bend between a horizontal pipe and a pipe inclined to the horizontal are investigated. Water is introduced into the upper leg and flows downward while the air injected into the horizontal leg flows countercurrently. The flow patterns are visualized. The different mechanisms which lead to flooding and are dependent on the water flow rate are observed. For low and intermediate water flow rates, the onset of flooding appears simultaneously with the slugging of unstable waves which are formed at the crest of the hydraulic jump. At low water flow rates, slugging appears close to the bend. At higher water flow rates it appears far away from the bend in the horizontal section. For high water flow rates, no hydraulic jump is observed and flooding occurs as a result of slug formation at the water flow outlet close to the end of the horizontal pipe.

Acknowledgements—The author wishes to thank Professor Dr.-Ing. D. Mewes and the staff of the Institute of Chemical and Process Engineering (Institut für Verfahrenstechnik), University of Hannover for their tremendous assistance during this work.

REFERENCES

Bankoff, S. G. & Lee, S. C. 1983 A comparison of flooding models for air–water and steam–water flow. In *Advances in Two-phase Flow and Heat Transfer* (Edited by Kakac, S. & Ishii, M.), Vol. 2, pp. 745–780. NATO ASI Series.

Gardner, G. C. 1983 Flooded countercurrent two-phase flow in horizontal tubes and channels. *Int. J. Multiphase Flow* **9,** 367–382.

Kawaji, M., Thompson, L. A. & Krishnan, V. S. 1989 Countercurrent flooding in an elbow between a vertical pipe and a downwardly inclined pipe. NURETH-4, Karlsruhe, Germany, pp. 20–27.

Krowlewski, S. W. 1980 Flooding limits in a simulated nuclear reactor hot-leg. B.Sc. thesis, Massachusetts Institute of Technology, Cambridge, MA, U.S.A.

Lee, S. C. & Bankoff, S. G. 1983 Stability of steam–water countercurrent flow in an inclined channel: flooding. *J. Heat Transfer* **105,** 713–718.

Ohnuki, A., Adachi, H. & Murao, K. 1988 Scale effects on countercurrent gas–liquid flow in a horizontal tube connected to an inclined riser. *Nucl. Engng Des.* **107,** 283–294.

Siddique, H., Ardron, K. H. & Banerjee, S. 1986 Flooding in an elbow between a vertical and a horizontal or near horizontal pipe, Part 1: experiment. *Int. J. Multiphase Flow* **2,** 531–541.

Wallis, G. B. & Dobson, J. E. 1973 The onset of slugging in horizontal stratified air–water flow. *Int. J. Multiphase Flow* **1,** 173–193.

Wan, P. T. 1986 Countercurrent steam–water flow in an upright 90° elbow. *Eighth International Conference in Heat Transfer* (Edited by Tien, C. L., Carey, V. P. & Ferrel, J. K.), San Francisco, pp. 2313–2318.